PHYSICAL REVIEW A **67**, 010501(R) (2003)

Precision measurement of the metastable $^3P_2$ lifetime of neon

Martin Zinner, Peter Spoden, Tobias Kraemer, Gerhard Birkl,* and Wolfgang Ertmer
Institut für Quantenoptik, Universität Hannover, Welfengarten 1, D-30167 Hannover, Germany
(Received 23 August 2002; published 30 January 2003)

The lifetime of the metastable $^3P_2$ state of neon has been determined as 14.73(14) s [decay rate 0.067 90(64) s^{-1}] by measuring the decay in fluorescence of an ensemble of ^{20}Ne atoms trapped in a magneto-optical trap (MOT). Due to low background gas pressure ($p<5\times10^{-11}$ mbar) and low relative excitation to the $^3D_3$ state (0.5 % excitation probability) only small corrections have to be included in the lifetime extrapolation. Together with a careful analysis of residual loss mechanisms in the MOT a lifetime determination to high precision is achieved.

DOI: 10.1103/PhysRevA.67.010501 PACS number(s): 32.70.Cs, 32.70.Fw, 32.80.Pj

In contrast to its importance for various active fields of research covering such a wide range as atomic physics, quantum optics, and nuclear physics, there still has been no measurement of the natural lifetime of the metastable $^3P_2$ state [1] of neon with sufficient precision. A selection of research activities profiting from an improved measurement include the quest for Bose-Einstein condensation (BEC) of metastable neon, advanced atomic structure calculations, the investigation of ultracold collisions, and even precision tests of the electroweak theory being currently persued by investigating the nuclear decay of an optically trapped sample of ^{19}Ne in the $^3P_2$ state [2].

Ongoing research directed towards BEC of metastable neon atoms in the $^3P_2$ state [3,4] clearly will benefit from an accurate knowledge of the state's lifetime. This includes the optimization of the production process as well as the study of collision processes such as Penning ionization [5] and elastic *s*-wave scattering. Exciting new physics complementing the work on metastable helium [6,7] can be expected for a $^3P_2$ neon condensate. We would like to mention in specific the study of higher-order correlations [8] and the intriguing possibility of a modification of the $^3P_2$ decay rate due to the high phase-space density or the phase coherence in a BEC [9].

Significant advance in atomic structure calculations has already been and will be further triggered [10] by the work presented here. To date only a preliminary experimental value of 22 s for the $^3P_2$ lifetime of neon exists [11] and no detailed investigations have been performed [12]. A precise determination of the lifetime will put a more stringent test on theory. For most rare-gas atoms, the $^3P_2$ lifetime depends sensitively on electron correlations and relativistic corrections. The latter have only a minor effect for the case of neon, making neon specifically interesting for a critical test of electron correlations. In addition, our measurement closes the chain of $^3P_2$ lifetime measurements for rare-gas atoms beyond helium performed in recent years for Ar (38^{+8}_{-5} s [13]), Kr (39^{+5}_{-4} s [13] and $28.3^{+1.8}_{-1.8}$ s [14]), and Xe ($42.9^{+0.9}_{-0.9}$ s and $42.4^{+1.3}_{-1.3}$ s [15]), respectively. This will deliver the input for a detailed systematic investigation of the Z dependence of metastable lifetimes.

An accurate experimental determination of the $^3P_2$ lifetimes of rare-gas atoms other than helium has only been achievable by the ability to prepare cold atom samples in a magneto-optical trap (MOT) [11,13,15,14]. For a precision lifetime measurement, the coupling of the $^3P_2$ to the $^3D_3$ state by the MOT light has to be considered since it will modify the observed decay rate. To date, two different methods making use of a variable MOT on-off duty cycle have been employed, either by directly measuring the rate of UV photons produced by the decay during a MOT-off period [15,14] or by extrapolating the observed decay rate for varying MOT on-off duty ratios to vanishing MOT-on periods [13].

In our approach, not requiring variable MOT on-off cycles, we record the decay of fluorescence in a MOT (Fig. 1) for different steady-state values of the population π_3 of the $^3D_3$ state ($0.005<\pi_3<0.47$). This allows the extrapolation of the observed decay rate to $\pi_3=0$, thus, giving the $^3P_2$ lifetime. Extreme care has been taken to achieve optimized experimental conditions such as low background gas pressure ($p<5\times10^{-11}$ mbar) and MOT operation for such

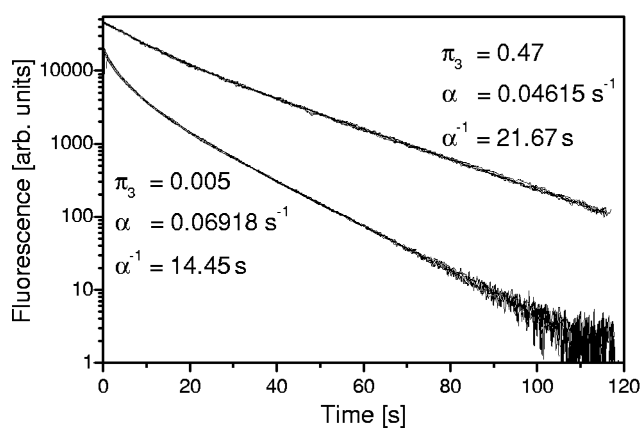

FIG. 1. Decay of the fluorescence for a ^{20}Ne ensemble in a MOT for the given excitations to the $^3D_3$ state of $\pi_3=0.005$ ($\Delta/\Gamma=-5.3$, $I/I_0=1.75$, $p=3.0\times10^{-11}$ mbar) and $\pi_3=0.47$ ($\Delta/\Gamma=-0.16$, $I/I_0=24$, $p=4.3\times10^{-11}$ mbar). Both sets of data consist of five curves each, demonstrating the high reproducibility of our decay measurements. The higher initial atom density for $\pi_3=0.005$ as compared to $\pi_3=0.47$ causes a higher initial nonexponential two-body decay.

*Author to whom correspondence should be addressed.

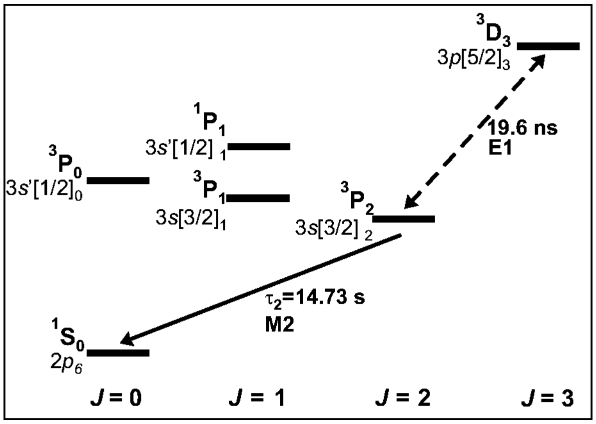

FIG. 2. Detail of the level scheme of neon. Atomic levels are labeled according to *LS* coupling and Racah notation. Transitions are labeled by their multipolar character.

low values as $\pi_3=0.005$. This minimizes the amount of required corrections dramatically and the accuracy to which the $^3P_2$ lifetime of Ne can be determined is improved considerably.

With no observable changes in shape and temperature of the atom sample, the temporal evolution of the observed fluorescence is proportional to the temporal evolution of the number of trapped atoms $N(t)$. The decay can be described by the differential equation

$$\frac{d}{dt}N(t)=-\alpha N(t)-\beta\int n^2(r,t)d^3r+O(n^3). \qquad (1)$$

The experimental fluorescence data is fitted to a solution of this equation. No absolute calibration of the atom number is required for the determination of the decay constant α. In Fig. 1, nonexponential two-body decay due to intratrap collisions can be seen during the first 30 seconds. Two-body losses depend on the integral over the local number density $n(r,t)$ and are described by the parameter β, the absolute determination of which would require an absolute calibration of $n(r,t)$, which is not the scope of this work. An uncalibrated value of β, however, is determined in our fitting procedure. For all data runs no contributions of order n^3 or higher could be observed.

At low atom numbers the decay is dominated by one-body losses with rate

$$\alpha=\frac{1}{\tau_2}(1-\pi_3)+\frac{1}{\tau_3}\pi_3+\gamma p+\mathcal{L}_M. \qquad (2)$$

The parameter π_3 gives the population in the $^3D_3$ state (see Fig. 2). Thus, $(1-\pi_3)N$ atoms decay from the $^3P_2$ state with lifetime τ_2. The combined rate for all decay channels from the $^3D_3$ state other than the transition to the $^3P_2$ state is given by τ_3^{-1}. Background collisions contribute with a rate of γp with p being the pressure in the vacuum chamber and γ being a constant depending on the atomic and molecular species present [16]. The parameter $\mathcal{L}_M$ summarizes possible MOT losses. The main objective of this work is to determine the lifetime τ_2 from the observed decay rates α by extrapolating to vanishing excitation $(\pi_3=0)$, background pressure $(p=0)$, and MOT losses $(\mathcal{L}_M=0)$. Achieving optimized starting conditions (small π_3 and p) and minimizing potential contributions of $\mathcal{L}_M$ by a systematic analysis of the MOT characteristics have been essential.

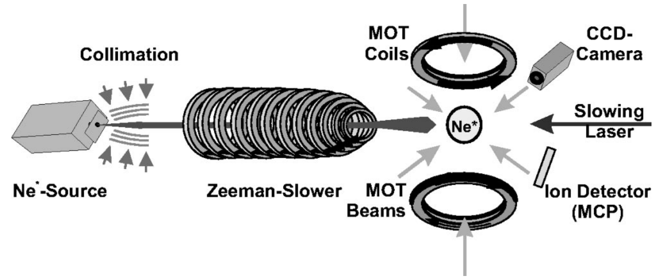

FIG. 3. Experimental setup.

Following [17], the population π_3 is determined by:

$$\pi_3=\frac{1}{2}\,\frac{CI/I_0}{1+CI/I_0+(2\Delta/\Gamma)^2}, \qquad (3)$$

with the total intensity I of the MOT light fields, the saturation intensity $I_0=\pi hc\Gamma/3\lambda^3=4.08$ mW/cm^2 (linewidth $\Gamma=2\pi\times8.18$ MHz, $\lambda=640.4$ nm), and detuning Δ. The phenomenological parameter C accounts for the deviation of the effective total intensity in a three-dimensional MOT from a one-dimensional two-level system [17]. We adopt the notion of Ref. [3] and take $C=0.7$ with an uncertainty of 0.3. The intensity I is measured with an uncertainty of 10%, the detuning Δ with an absolute uncertainty of 1 MHz. Therefore, for all data presented here the uncertainty in C is the dominant contribution to the uncertainty in π_3.

The experimental setup is shown in Fig. 3. A collimated beam of metastable atoms is decelerated in a Zeeman slower with the slowing laser beam passing through the center of the MOT. The MOT light field consists of six individual beams (diameter 22 mm) with spatially filtered beam profiles. All light fields are derived from a dye laser which is frequency stabilized to a neon rf discharge.

For each run, the MOT is loaded for 400 ms reaching a number of up to 4×10^8 atoms, a maximum collision-limited density of the order of 1×10^9 cm^{-3} and a typical temperature below 1 mK. Then, the loading process is terminated by blocking the atomic beam and the slowing laser beam by mechanical shutters, and by switching off the magnetic field of the Zeeman slower. In the following measurement period of two minutes, the fluorescence of the trapped atoms is recorded by a charge-coupled device camera capturing five image frames per second. Fluorescence decay curves are obtained by integrating the counts of each frame over the region where atoms are present. Great care has been taken to eliminate the influence of residual stray light. The decay curves span up to four orders of magnitude in signal. Figure 1 shows two sets of data taken for different values of π_3. For $\pi_3=0.005$ a decay rate of $\alpha=0.069\,18(51)$ s^{-1} and a respective decay time of $\alpha^{-1}=14.45$ s is observed.

In the following sections, we describe our procedure to extrapolate the observed decay rate α to the $^3P_2$ decay rate

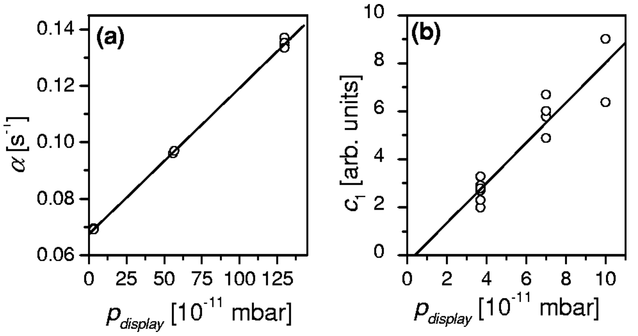

FIG. 4. (a) Decay rates α obtained for $\pi_3 < 0.02$ as a function of the nominal background pressure $p_{display}$. (b) Coefficients c_1 proportional to the number of ionizing background collisions as a function of $p_{display}$ allowing the determination of the vacuum gauge offset.

τ_2^{-1}. For the extrapolation of α to vanishing background pressure a systematic investigation of the MOT decay as a function of pressure has been carried out [Fig. 4(a)] by heating or cooling a section of the vacuum chamber. The pressure is given as the nominal reading of the vacuum gauge (Balzers IKR070). The specific composition of the background gas is not known. However, we could observe a linear dependence of α on pressure over a range of almost two orders of magnitude, indicating a pressure-independent composition of the background gas. From a linear fit for data taken for $\pi_3 < 0.02$, we can determine the slope $\gamma = 5.2(1) \times 10^7\ \mathrm{mbar}^{-1}\,\mathrm{s}^{-1}$. As a special feature of our setup, we can directly determine a possible offset by simultaneously measuring the fluorescence and the rate of ions produced by collisions using a multichannel plate (MCP) ion detector. Under typical operating conditions, we detect ions of different origin: (a) Ne^+ ions originating from intratrap collisions [rate $\propto \int n^2(r,t) d^3 r$]. (b) Ions which originate from collisions of metastable neon atoms with residual gas constituents [rate $\propto N(t) \times p$]. Thus, the ion count rate $R_{\mathrm{ion}}(t)$ can be modeled by

$$R_{\mathrm{ion}}(t) = c_1 N(t) + c_2 \int n^2(r,t) d^3 r, \tag{4}$$

where c_1 is assumed to be proportional to p. The values of c_1 obtained for different pressures are shown in Fig. 4(b). From a linear fit, we can determine the offset of the pressure gauge reading to $(4 \pm 7) \times 10^{-12}$ mbar also allowing for a vanishing offset. By combining the results for γ and the offset, we can extrapolate the observed decay rates to $p = 0$. Due to the already low background pressure for our decay measurements only small corrections arise; at $p = 3 \times 10^{-11}$ mbar the background collision rate of $\gamma p = 1/(640\,\mathrm{s})$ is more than a factor of 40 smaller than the observed decay rate α.

We also investigated the possibility of additional atom losses from the MOT [contribution $\mathcal{L}_M$ in Eq. (2)] attributed to a finite trap depth U_0 or finite escape velocity v_e [18]. We assume that an infinite trapping volume leading to infinite U_0 and v_e would result in a lossless MOT. In principle, this could be achieved for the applied magnetic-field gradient B'

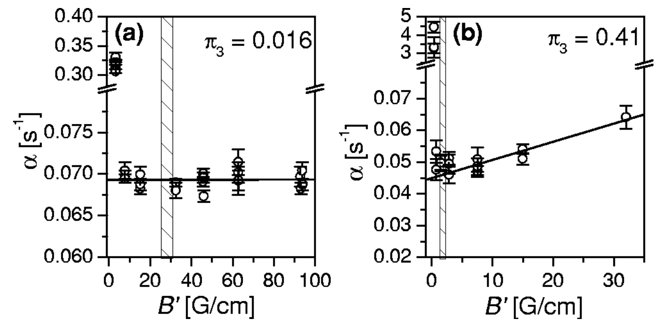

FIG. 5. Systematic investigation of MOT losses. Decay rates are plotted as a function of the magnetic-field gradient for two different excitations (a) $\pi_3 = 0.016$ and (b) $\pi_3 = 0.42$. Shaded areas indicate the gradients of typical operating conditions.

approaching zero if the MOT beams could be made infinitely large. In all practical implementations the trap depth will remain finite due to the finite size of the laser beams. Thus, for a given beam geometry, a variation in B' should allow to investigate the MOT stability and to quantify the MOT losses $\mathcal{L}_M$ which include diffusive motion out of the trapping volume [19] leading to an exponentially decreasing loss rate with increasing trap depth and nonionizing background gas collisions [16] already being accounted for by the $p \to 0$ extrapolation.

The influence of the magnetic-field gradient on the measured decay rate α is shown in Fig. 5 for two values of $\pi_3 = 0.016$ and 0.41, respectively. In the most relevant case of small π_3 [Fig. 5(a)], for sufficiently large $B' > 10$ G/cm a variation of B' does affect the measured α not more than the uncertainties obtained from the fit. Thus, we conclude that for our operating regime [shaded region in Fig. 5(a)] the trap depth U_0 and escape velocity v_e are sufficiently large and that potential MOT loss contributions to the decay rate α are not significant.

For large π_3 [Fig. 5(b)], a variation of the MOT stability with B' is observed. No quantitative model of the MOT at high saturation exists, the application of the loss models discussed above is not straightforward, and only a minimum and a maximum estimate of $\mathcal{L}_M$ can be given; since our decay data for large π_3 have been taken at $B' = 1.5$ G/cm

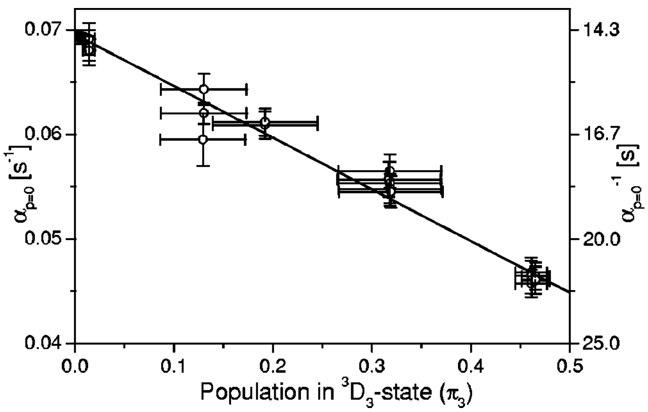

FIG. 6. Decay rates $\alpha_{p=0}$ as a function of the excitation π_3 allowing the determination of τ_2 in the limit of $\pi_3 \to 0$.

TABLE I. Contributions to the $\tau_2 = 14.73(14)$ s extrapolation. Uncertainties are given by the quadrature sum of individual contributions, either systematical or statistical.

	Contribution (s^{-1})	Uncertainties (s^{-1})
MOT decay at $\pi_3 = 0.005$	0.06918	± 0.00051
$p \to 0$ extrapolation	-0.00156	± 0.00037
$\pi_3 \to 0$ extrapolation	$+0.00028$	± 0.00013
$1/\tau_2$	0.06790	± 0.00064

which gives the best MOT stability, MOT losses might not have a significant contribution on the determination of α at all. On the other hand, a linear extrapolation of α to $B' = 0$ gives an upper limit of $\mathcal{L}_M = 0.005(2)\ s^{-1}$ but should overestimate the corrections to be made [19,16]. Since losses for large π_3 only influence the slope of the $\pi_3 \to 0$ extrapolation, we take them into account by incorporating $0\ s^{-1} < \mathcal{L}_M < 0.005\ s^{-1}$ for large π_3 into the uncertainties of this extrapolation.

After this systematic study of the influence of background collisions and MOT losses the determination of the $^3P_2$ lifetime τ_2 can be obtained by extrapolating the measured decay rates to vanishing population π_3. Only data for a pressure below 5×10^{-11} mbar are considered and an extrapolation to $p = 0$ is performed. The dependence of the resulting rates $\alpha_{p=0}$ on π_3 is shown in Fig. 6 exhibiting a simple linear behavior. Displayed uncertainties in $\alpha_{p=0}$ are given by the combined statistical and systematic uncertainties in the fit of α and in the $p \to 0$ extrapolation. To minimize uncertainties in the $\pi_3 \to 0$ extrapolation, only datasets for $\pi_3 < 0.05$ and $\pi_3 > 0.4$ showing the smallest absolute uncertainties in π_3 have been included. The final value of the $^3P_2$ lifetime and decay rate are $\tau_2 = 14.73(14)$ s and $\tau_2^{-1} = 0.06790(64)\ s^{-1}$, respectively. Table I gives a summary of contributions and uncertainties for these values. Since stable MOT conditions are directly accessible for $\pi_3 = 0.005$ and $p < 5 \times 10^{-11}$ mbar only unprecedented small corrections are required. The final value for τ_2 only deviates from the uncorrected value of $\alpha^{-1} = 14.45$ s by 2%.

In addition to this result, extrapolating $\alpha_{p=0}$ to $\pi_3 = 1$, that is, to a hypothetical total population transfer to the $^3D_3$ state, is also possible. From this, we gain the experimentally determined lower limit of $\tau_3 \geqslant 59$ s for the combined rate τ_3^{-1} of decay of the $^3D_3$ state via all channels except the direct decay to the $^3P_2$ state. However, this value depends sensitively on the $\mathcal{L}_M$ correction applied for large π_3 and only the stated lower limit is accessible.

To conclude, we would like to compare our result of $\tau_2 = 14.73(14)$ s to theoretical values obtained by different atomic structure calculations. Prior to our work, published theoretical values were given in Ref. [20] to 24.4 s, which can be rescaled to 20.0 s using more accurate input parameters, and in Ref. [21] to 22 s. Significant remaining discrepancies initiated a reexamination of atomic structure calculations for the whole set of $^3P_2$ lifetimes of rare-gas atoms. A preliminary result based on a multiconfiguration Dirac-Fock calculation gives a value of 18.9 s for neon [10]. A high degree of sensitivity to the included electron correlations has been found. Theoretical values are still expected to be larger than the experimental value, since the inclusion of additional electron correlations should further reduce the calculated lifetime. Refined calculations are forthcoming [10]. Most recent *ab initio* calculations using multiconfiguration Hartree-Fock methods give a lifetime of 16.9 s [22]. Considering the combined progress in experiment and theory, we anticipate that the determination of the $^3P_2$ lifetime of neon may continue to serve as an important test for precision atomic structure calculations in the future.

We thank Y.-K. Kim for valuable discussions and are grateful for financial support by the DFG within the *Schwerpunktprogramm SPP 1116*.

[1] The notation of states throughout this paper is based on *LS* coupling. Racah notation is included in Fig. 2.
[2] see, e.g., http://weak0.physics.berkeley.edu/weakint/research/neon/
[3] S.J.M. Kuppens *et al.*, Phys. Rev. A **65**, 023410 (2002).
[4] M. Zinner, Ph.D. thesis, Universität Hannover, 2002 (unpublished); http://www.iqo.uni-hannover.de/html/ertmer/atom_optics/nebec/nebec.html
[5] F.M. Penning, Naturwissenschaften **15**, 818 (1927).
[6] A. Robert *et al.*, Science **292**, 461 (2001).
[7] F. Pereira Dos Santos *et al.*, Phys. Rev. Lett. **86**, 3459 (2001).
[8] M. Yasuda and F. Shimizu, Phys. Rev. Lett. **77**, 3090 (1996); E.A. Burt *et al.*, *ibid.* **79**, 337 (1997); W. Ketterle and H.J. Miesner, Phys. Rev. A **56**, 3291 (1997).
[9] J.J. Hope and C.M. Savage, Phys. Rev. A **54**, 3177 (1996).
[10] J.P. Desclaux, P. Indelicato, and Y.-K. Kim (private communication).
[11] F. Shimizu, *Laser Spectroscopy IX* (Academic Press, New York, 1989), p. 444ff.
[12] F. Shimizu (private communication).
[13] H. Katori and F. Shimizu, Phys. Rev. Lett. **70**, 3545 (1993).
[14] J. Lefers *et al.*, Phys. Rev. A **66**, 012507 (2002).
[15] M. Walhout, A. Witte, and S.L. Rolston, Phys. Rev. Lett. **72**, 2843 (1994).
[16] A.M. Steane, M. Chowdhury, and C.J. Foot, J. Opt. Soc. Am. B **9**, 2142 (1992).
[17] C.G. Townsend *et al.*, Phys. Rev. A **52**, 1423 (1995).
[18] J. Weiner *et al.*, Rev. Mod. Phys. **71**, 1 (1999).
[19] P.A. Willems *et al.*, Phys. Rev. Lett. **78**, 1660 (1997).
[20] N.E. Small-Warren and L.-Y. Chow-Chiu, Phys. Rev. A **11**, 1777 (1975).
[21] J.P. Desclaux, P. Indelicato, and Y.-K. Kim, cited in Ref. [15].
[22] G. Tachiev and C. Froese Fischer, 2002, http://atoms.vuse.vanderbilt.edu